Transformer Modelling for the Frequency and Transient Analyses, with Non-Uniform Inductance Emulating the Inter-Turn Magnetic Coupling

Mohamed M. SAIED, IEEE Senior Member

Professor (Emeritus), Independent Researcher, Giza, Cairo, Egypt; m.saied@ieee.org

Summary: **A new procedure for analyzing power transformer windings with location-dependent circuit parameters, such as the series inductance, is presented. This dependence is introduced in order to take the inter-turn mutual inductive coupling into consideration. It can be expressed either by analytical expressions or even in a tabulated form. The paper addresses both the frequency and time domain analyses. They are based on replacing the winding by an adequate number of equivalent cascade connected two-ports. In contrast to the usual practice of applying the simple medium line representation, each of these two-ports is treated as a long transmission line. Their *A, B, C, D* generalized circuit constants will be therefore generally location-and frequency-dependent. The analyses will be conducted in the complex *s*-domain. The corresponding time-domain results can then be obtained by applying a numerical inverse Laplace transform. Expressions for the winding's input impedance with different treatments of the transformer's neutral point will be derived for any assumed number of the equivalent two-ports. Results pertinent to the frequency characteristics including the resonance frequencies are presented. The paper also describes the winding's transient response to the application of two standard voltage stimuli. The suggested approach is validated by its application to a case study for which an analytical closed-form solution is available. The analysis of windings exhibiting nonuniformities in more than one equivalent circuit element should also be possible.**

Key Words*:*
distributed parameter circuits,
frequency response,
modeling,
power system transients,
power transformers,
resonance,
non-uniform

I. INTRODUCTION

The time-domain and frequency-domain analyses are the two main approaches currently applied for finding the transients in transformer windings as well as the frequency response describing their internal oscillations and resonance phenomena, [1-14]. The frequency- (or, equivalently, the *s*-domain) approach assumes problem's linearity. With this limitation, it has been used for deriving analytical expressions for the voltages and currents within the transformer and for identifying the winding's resonance frequencies, [5-9]. Reference [10] is based on a concentrated parameter approach and presents a method for considering the non-uniformity of the winding's series inductance, due to the mutual inductive interaction between any winding turn and all other ones. The winding is divided into a suitable number of sections represented by their non-identical lumped ladder equivalent circuits. The simulation is then conducted by solving the corresponding set of simultaneous differential and algebraic equations in the Laplace domain. The model can be considerably refined by applying an alternative straight forward concentrated-parameter recursive *s*-domain analytical solution technique [11], as successfully used in [12] for analyzing transmission line towers. The simulation accuracy of the two above-mentioned approaches obviously increases with the assumed number of sections, which is limited by the available computational resources. This present paper suggested a more accurate and efficient approach. It is based on the distributed parameter analysis utilizing the *A, B, C, D* generalized circuit constants commonly used for simulating transmission lines. The proposed technique starts with replacing the winding by an adequate number of equivalent cascade connected two-ports. Each of these two-ports is treated as a long transmission line. This implies an improved accuracy if compared with the usual concentrated element representation. The *A, B, C, D* generalized circuit constants will be location- and frequency-dependent. The solution of the corresponding simultaneous algebraic two-port equations will yield the currents and voltages along the winding for any input stimuli as well as its input impedance, in the s-domain. As will be seen later, the suggested solution, augmented by the numerical inverse Laplace transform, lends itself quite well to both the transient and frequency analyses.

This paper is organized as follows: First, the basic concept is presented and the *s*-domain results are derived. This will be followed by its application to different case studies both in the frequency and the time domains. Before listing the paper's conclusions, the suggested technique is validated by its application to a case study for which an exact analytical closed-form solution is available.

II. METHOD OF ANALYSIS

Fig.1 illustrates the equivalent circuit of a winding section having a per unit length dx based on the winding's total length, which is measured from the source terminal in meters or turns. The depicted circuit elements are defined as follows:

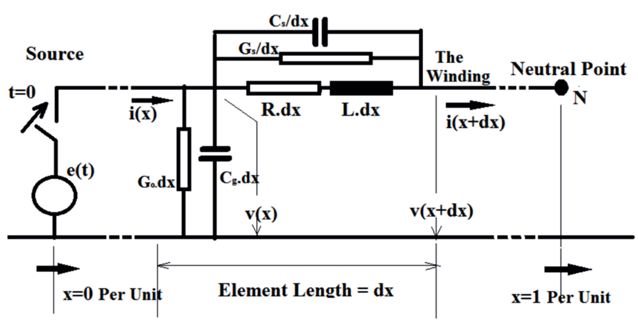

Fig.1. The winding representation and the equivalent circuit of an infinitesimal section of length dx.

C_g capacitance to ground
G_o Conductance to ground
L series inductance, which is a function of the coordinate x
R series resistance
C_s series (self) capacitance
G_S insulation conductance

It should be noted that the series inductance L is generally a function of the location x of the considered section. It takes into account the mutual inductances between the considered section at this location and the remaining ones. Since these mutual inductances decrease with the separation, the inductance L will assume its maximum value at the winding midpoint (x=0.5 per unit). A typical shape of this dependence is given in Fig. 2, adopted from reference [13] utilizing the evaluation of the Neumann's formula integrals for assessing the mutual inductive coupling between any two winding turns. It ranges between the least values of 0.014H at both winding terminals to the highest value of 0.028H at its midpoint. This dependence of L on the coordinate x can be approximated by:

$$L(x) = [L_{\min} + (L_{\max} - L_{\min}).\sqrt[3]{\sin(\pi x)}] \qquad (1)$$

It should be noted, however, that other candidate functions for expressing $L(x)$ can be adopted through curve fitting techniques.

The first step in the suggested technique for the winding analysis is to divide it into an adequate number of equivalent cascade connected two-ports, as shown in Fig.3. The source is represented by its Thevenin's equivalent circuit and the neutral treatment is expressed by the general frequency dependent $Z_N(s)$ The two special cases $Z_N(s)$=0 and $Z_N(s)$ =∞ describe the solidly-earthed and isolated neutral points, respectively. The corresponding inductance values are depicted in Fig.4 for m=16. In contrast to the usual practice of applying the simple medium line representation, each of these two-ports will be treated as a long transmission line. Their A, B, C, D generalized circuit constants will be therefore generally location- and frequency-dependent. The analyses will be conducted in the complex s-domain. Focusing on the n-th section, the x co-ordinates of its left and right side terminals are $(n–1)/m$ and (n/m) per unit, respectively. The average value of the two corresponding series inductances will be used in order to find the generalized circuit constants

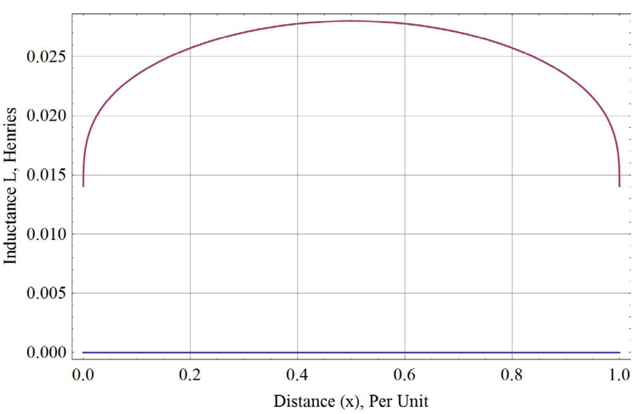

Fig. 2. Value of *L(x)* versus the coordinate x along the winding, [13].

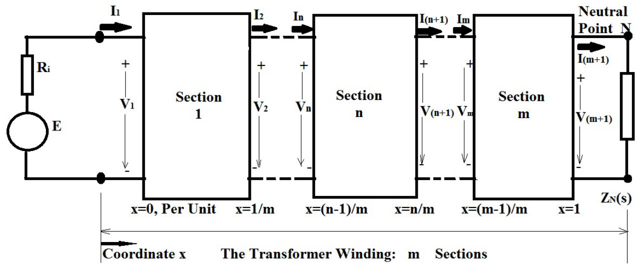

Fig. 3. Representing the winding by m cascaded sections of length (1/m) per unit each.

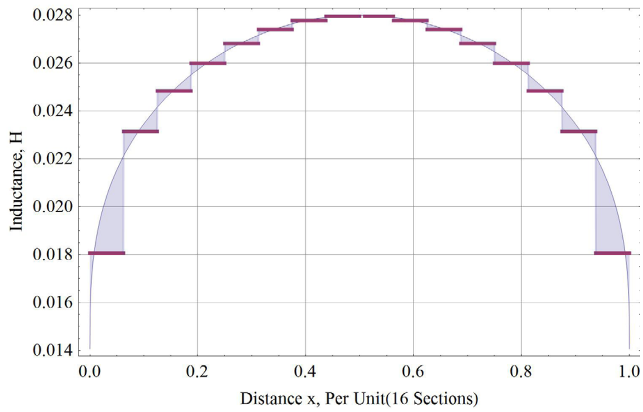

Fig. 4. The exact inductance values (continuous curve) and the assumed stepped curve for the average inductances. The assumed number of sections is m =16.

of this section. In terms of transmission line theory, the series impedance and shunt admittance per unit length are given by the following two equations

$$Z_{series} = [(sC_s + G_s) + (R + sL)^{-1}]^{-1} \qquad (2)$$

$$Y_{shunt} = sC_g + G_o \qquad (3)$$

The symbol s denotes the complex frequency.

The complex characteristic impedance and propagation constant of the equivalent line are defined as $\gamma = \sqrt{Z_{series} Y_{shunt}}$ and $Z_C = \sqrt{Z_{series} / Y_{shunt}}$,respectively. In the s-domain, the transmission line constants are:

$$A = D = \cosh(\gamma l)$$

$$B = Z_C \sinh(\gamma l) \qquad (4)$$

$$C = \sinh(\gamma l) / Z_c$$

with the section length l = 1/m per unit.

It should be noted that the inductance L in Eq. (2), and accordingly, γ, Z_C, A, B, C and D are all functions of the location x (or equivalently the section number n) and of the complex frequency s.

For the steady state sinusoidal analysis, s should be replaced by $j\omega$, where ω is the angular frequency and $j = \sqrt{-1}$. The plots in Fig.5 show the magnitudes of the generalized constants A, B and C at 20 kHz for a transformer having the following circuit parameters adopted from [13]:

$$C_s = 2.07 \text{ pFarad}, \; C_g / C_s = 10000, \; G_o = 0.15 \text{ nSiemens},$$
$$R = 2.198\ \Omega \text{ and } G_s = 0.15 \text{ pSiemens};$$

It can be seen that the three plots in Fig.5 are almost symmetrical with respect to the winding's middle point $n = m/2 = 8$ at which A, C and D have their least values and B assumes its maximum value, respectively. The changes in these constants at 20 kHz are about 0.6%, 36% and 5%, respectively.

Referring to Fig.3, the two following equations can be written for the Section of number n:

$$V_m = A_m V_{m+1} + B_m I_{m+1} \quad \text{and} \quad I_m = C_m V_{m+1} + D_m I_{m+1} \quad (5)$$

Repeating this for all the m sections, and adding the two loop equations at the source and at the neutral point, a total number of ($2m$+2) equations will be available. All currents and voltages can then be obtained in terms of the complex frequency s, for any exciting source voltage $E(s)$ and any neutral impedance $Z_N(s)$.

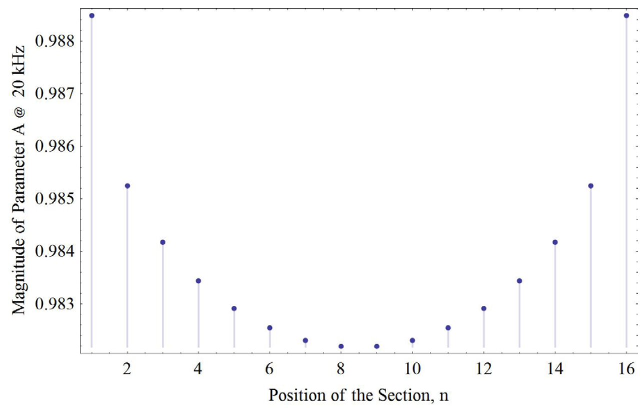

(a) The Magnitude of both A and D

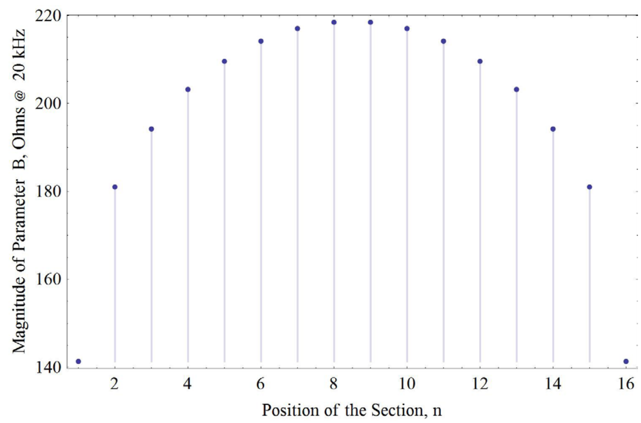

(b) The Magnitude of B

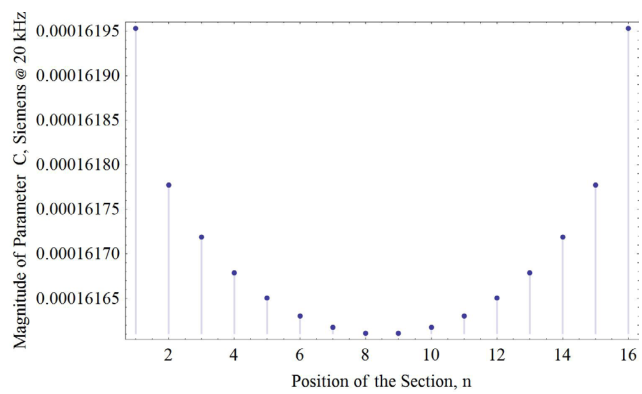

(c) The Magnitude of C

Fig. 5. The magnitudes of the constants A, B and C for the different 16 sections at 20 kHz.

III. SAMPLE RESULTS

A. The Frequency Response

This section will focus on the winding's input impedance as seen from the source side. It is given by:

$$Z_{input}(s) = V_1(s) / I_1(s) \quad (6)$$

where $V_1(s)$, $I_1(s)$ are the voltage and current at the left hand side (input) terminals of the first section, i.e. n = 1. It will depend primarily on both the frequency as well as on the winding's neutral impedance $Z_N(s)$.

1. Isolated Neutral

The upper four plots of Fig. 6 illustrate the effect of the frequency f, given in kHz on the x-axis, on the impedance magnitude, its impedance angle in degrees, its imaginary part and its real part, from top to bottom, respectively. The traces cover the frequency range $0 \le f \le 250$ kHz. As expected, the DC input impedance is infinity. There are several series and parallel resonance frequencies which can be easily determined from the zero crossings of either the phase angle or the impedance imaginary part. The lowest resonance frequency of approximately 12 kHz is a series one followed by a parallel resonance at about 24 kHz. Between zero and 12 kHz, the impedance is seen to be resistive/capacitive.

The two plots 6-(e) and 6-(f) depict the locus diagrams of the winding's input impedance over the frequency range $0 \le f \le 100$ kHz. They are parametric plots for the complex impedance as the frequency changes within these limits. The plot (e) illustrates the case of nonuniform winding while the second one shows the hypothetical case of a uniform winding of $L(x)$ = 0.021mH. Each of the circles represents a combination of a series and parallel resonances. In both plots, there are little differences between the impedance magnitudes at the series resonance frequencies. In the base case of nonuniform inductance, the impedance magnitudes at

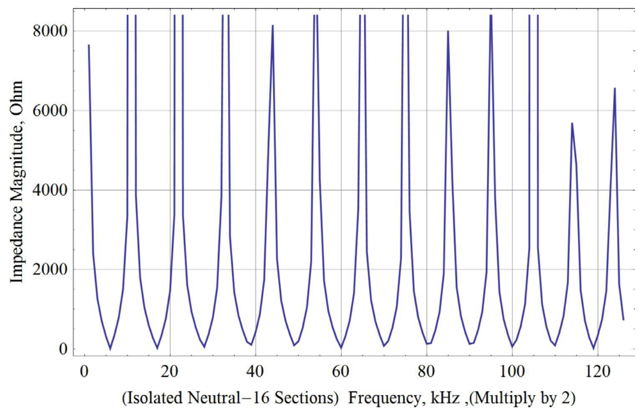

6 – (a)

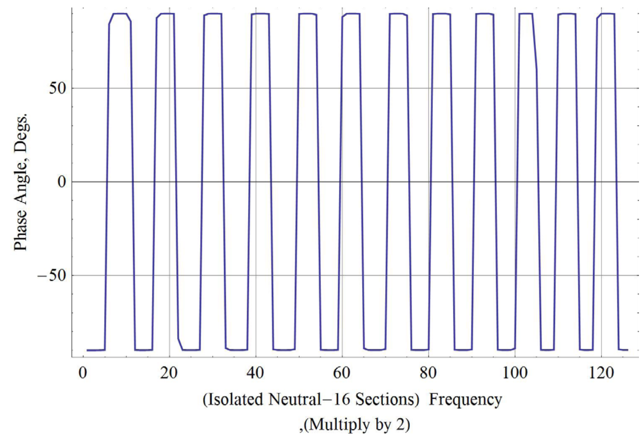

6 – (b)

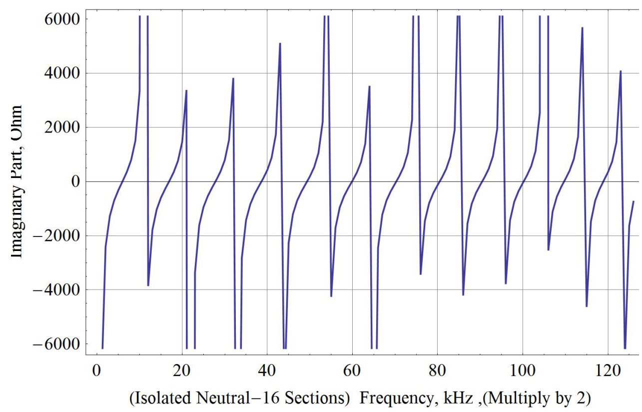

6 – (c)

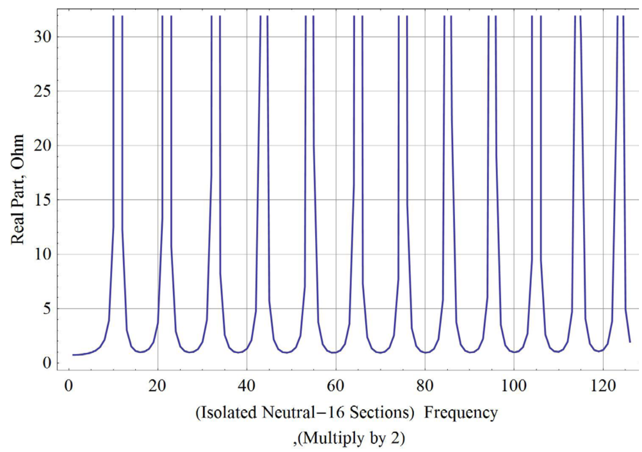

6 – (d)

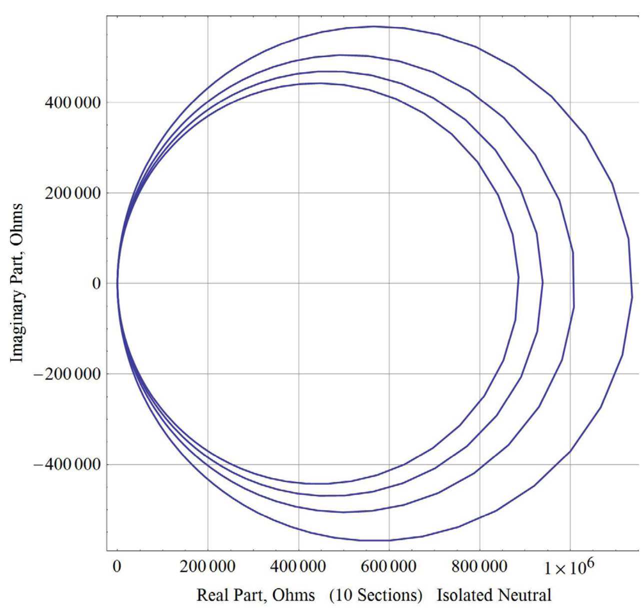

6 – (e)

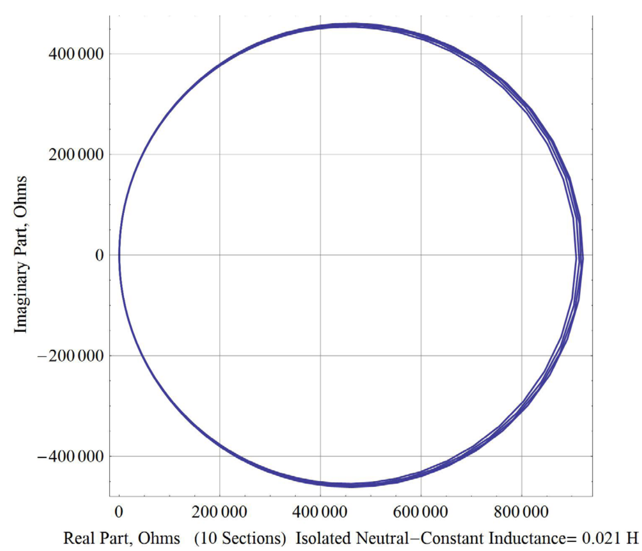

6 – (f)

Fig. 6. The winding’s input impedance versus the frequency for the case of isolated neutral

the parallel resonance frequencies vary in four discrete steps between about 0.875 and 1.125 MΩ. In the case of uniform inductance, however, these differences in the impedance magnitudes are much smaller, as seen in plot 6-(e).

2. Solidly-Earthed Neutral

Fig.7 depicts the results for the case of solidly-earthed neutral. The DC input impedance is seen from the curves as a pure resistance of about 2.2 Ω. This is equal to the previously assumed winding ohmic resistance *R*. The lowest resonance frequency is a parallel one close to 12 kHz. At very low frequencies, the winding exhibits an inductive imaginary part, which increases almost linearly with the angular frequency. The proportionality constant is about 25mH, which is close to the average value of the assumed inductance curve in Fig.2. This is clearly recognizable by inspecting the plot at the bottom giving the impedance magnitude over the low frequency range $0 \leq f \leq 1$ kHz.

As shown by the plot 7-(f), the impedance magnitudes at the parallel resonance frequencies vary in five discrete steps between about 0.840 and 1.125 MΩ. Similar to plot 6-(f) for isolated neutral, the differences in the impedance magnitudes are much smaller if the winding's inductance is assumed uniform.

3. Inductively-Earthed Neutral

The plots given in Fig.8 illustrate the frequency characteristics of the winding if its neutral is earthed via a lossless Petersen coil of inductance 50 mH. The value $Z_N(s) = 0.05\ s$ is substituted in the model equations. The first resonance (at about 5 kHz), which is a parallel one, occurs at a lower frequency compared to the previous case of solid earthing.

The two locus plots 8-(d) and 8-(e) illustrate the winding's input impedance over the frequency range $0 \leq f \leq 100$ kHz with and without taking the inductance nonuniformity into account, respectively. In this case an additional parallel resonance of much larger input impedance (approximately 4.2MΩ) can be recognized. The computed frequency of this anti-resonance is about 4.595 kHz. It is close to the parallel resonance frequency (4.152 kHz) of the winding's approximate low frequency equivalent circuit. It is composed

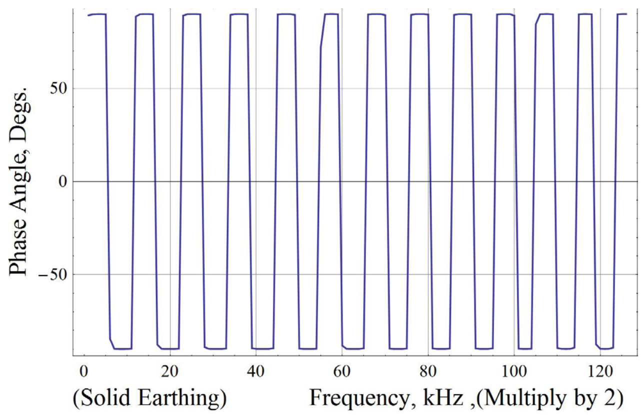

7 – (b)

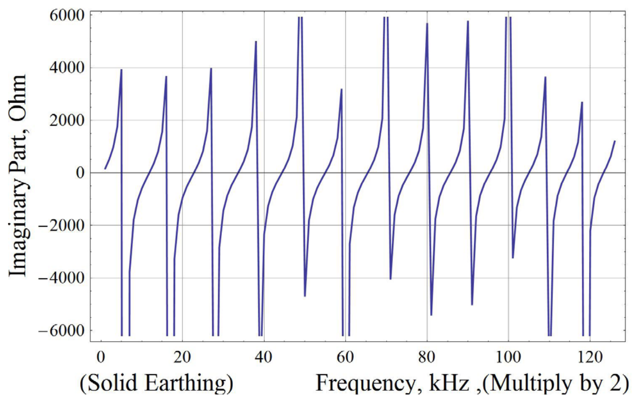

7 – (c)

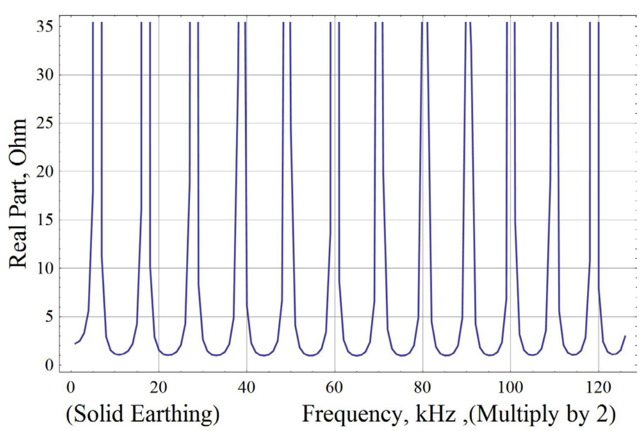

7 – (d)

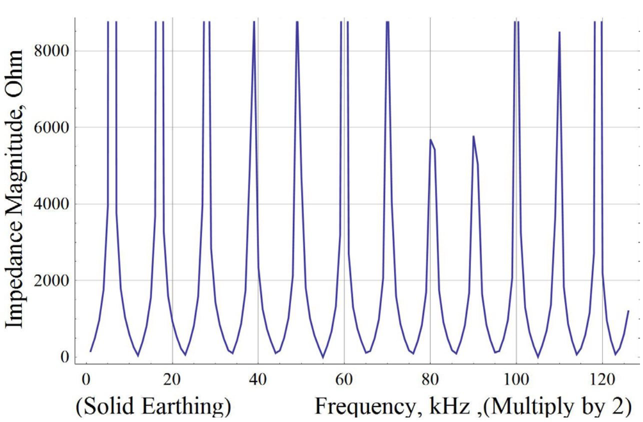

7 – (a)

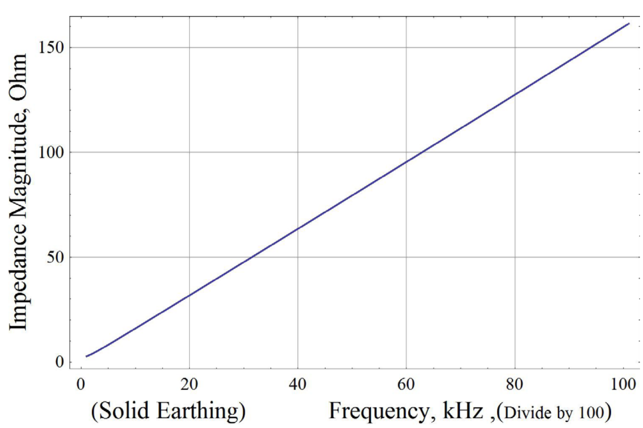

7 – (e)

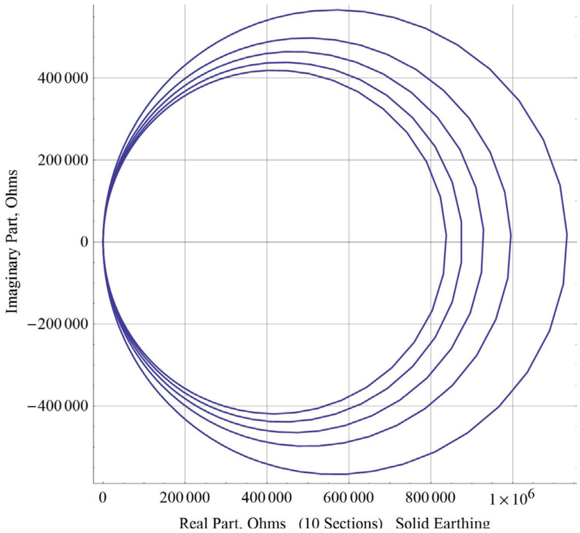

7 – (f)

Fig. 7. The winding's input impedance as a function of the frequency for solidly-earthed neutral.

of the earth capacitance C_g in parallel with the branch composed of the series connection of the winding resistance and the average total inductance of about (0.021+0.05) H.

4. Resistively-Earthed Neutral

Results pertinent to the case of the transformer winding with a 10-Ohm neutral resistance are illustrated by the plots of Fig.9. The lowest resonance is a parallel one occuring at about 11 kHz followed by a seies resonance frequency

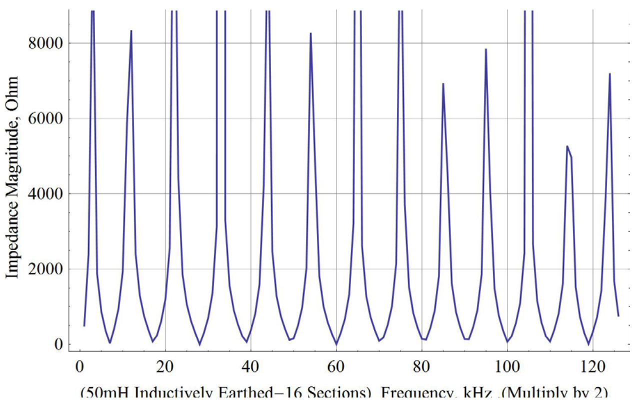

8 – (a)

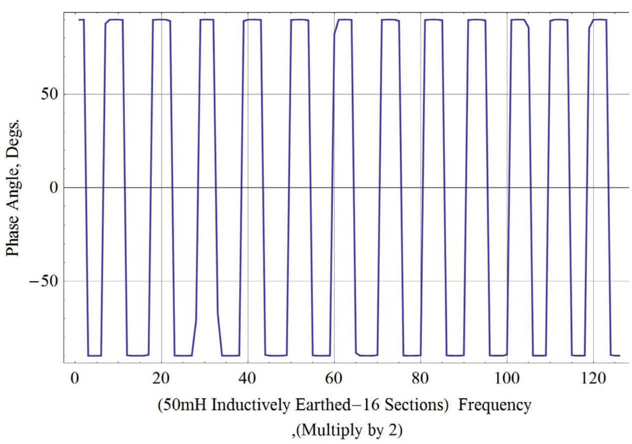

8 – (b)

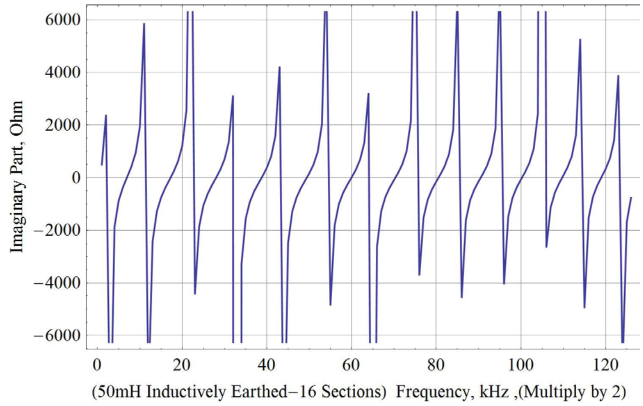

8 – (c)

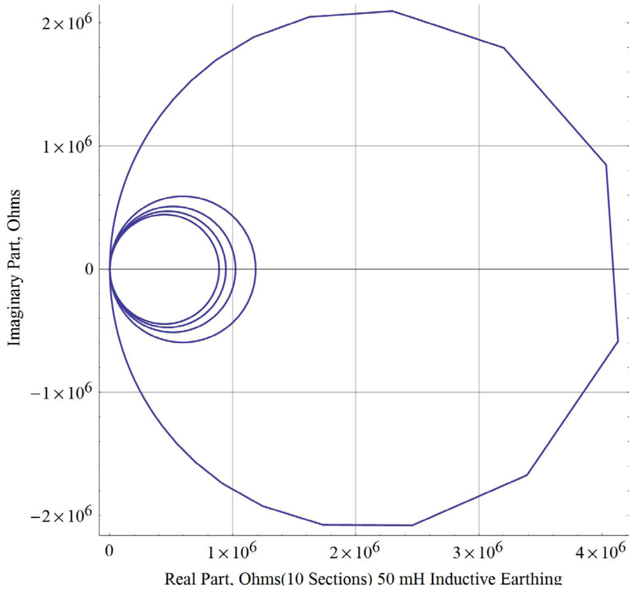

8 – (d)

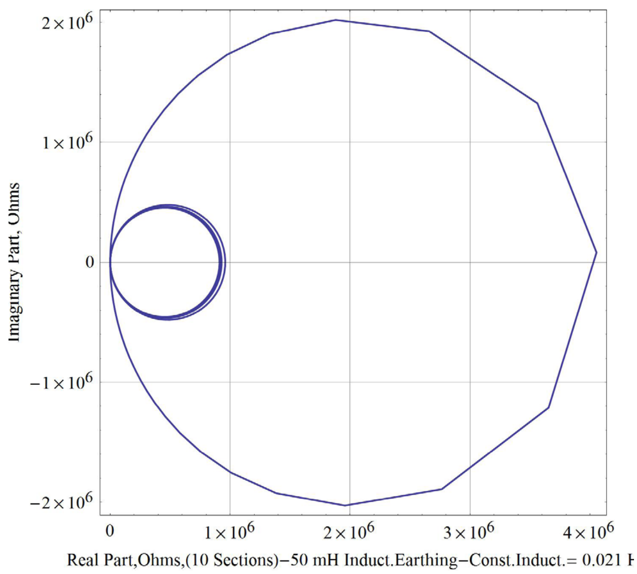

8 – (e)

Fig. 8. Dependence of the winding's input impedance on the frequency for inductively-earthed neutral via a lossless 50 mH Petersen coil.

close to 23 kHz . For DC, the plot of the real part indicates an input resistance of about 12.20 Ohms, as expected. As the impedance locus diagram 9-(c) indicates, the expected maximum impedance values at the parallel resonance frequencies are generally smaller than those of the other cases of neutral treatment. This is attributed to the increased ohmic dissipation introduced by the neutral resistance which leads to less selective resonances, i.e. of lower values of resonance quality factors.

By inspecting the above results for the different transformer's neutral treatments, the magnitude of the input impedance ranges from a few Ohms at the series resonance frequencies to large values between about 70 kΩ and 4.2 MΩ at parallel resonance.

B. The Transient Response

This section is intended to demonstrate the application of the suggested approach to determine the transient response of the transformer winding to the switching of a voltage source. The internal resistance of the source is assumed $R_i = 20\Omega$.The results will be given for both double-exponential impulse and step voltage sources expressed by $e(t)$ in Fig.3. The transient response of the voltage $v(x,t)$ and current $i(x,t)$ at any point of co-ordinate x is computed using the Hosono algorithm for the numerical inverse Laplace transform, successfully applied in [5–9].

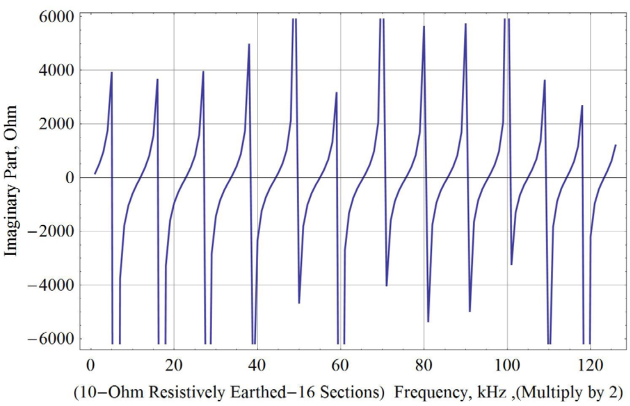

9 – (a)

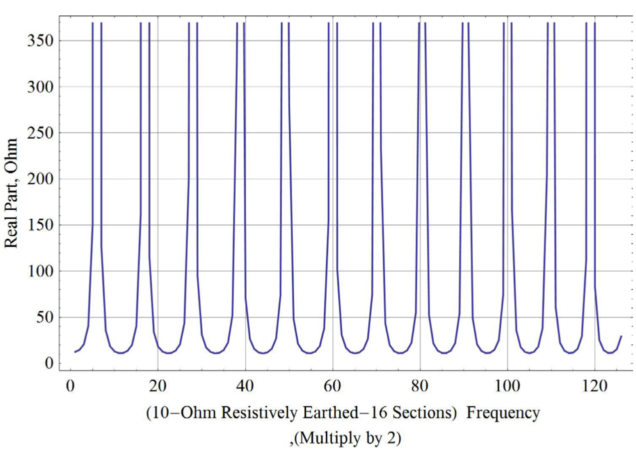

9 – (b)

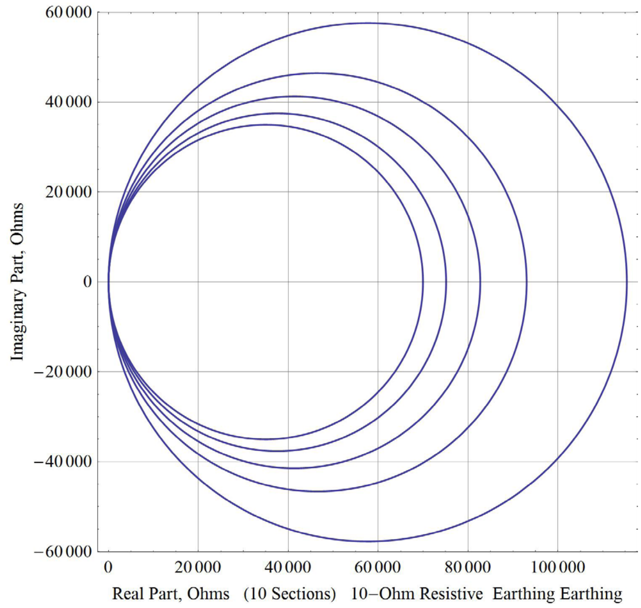

9 – (c)

Fig. 9. The winding's input impedance as a function of the frequency for the transformer winding when resistively-earthed via a 10-Ohm neutral resistance.

1. Transients Due to a Double-Exponential Impulse Voltage

A voltage impulse of the following waveform is assumed for the source EMF, with t expressing the time in seconds:

$$e(t) = 1037[e^{-(\frac{10^6 t}{68.5})} - e^{-(\frac{10^6 t}{0.405})}] \quad (7)$$

This equation, illustrated by the upper plot (a) of Fig.10, represents an impulse of a crest value 1000V, approximate front and tail times 1.5 and 50µsec, respectively.
Its Laplace transform $E(s)$ is available in standard tables.
In the s-domain, the current and voltage at the transformer's input terminal (I_1 and V_1 in Fig. 3, respectively) are given by:

$$I_1(s) = E(s)/[R_i + Z_{input}(s)] \quad (8)$$

$$V_1(s) = E(s) - R_i.I_1(s) = I_1(s).Z_{input}(s) \quad (9)$$

The current I_2 and voltage V_2 at the junction between the two sections 1 and 2 in Fig.3 can then be derived from the equations

$$I_2 = D_1 I_1 - C_1 V_1$$

and (10)

$$V_2 = A_1 V_1 - B_1 I_1$$

This can be successively repeated for the other sections.

Due to the relatively large value of the assumed capacitance to ground, C_g , the initial value of the winding's input impedance will be close to $\sqrt{L_{min}/C_g} \approx 822\,\Omega$, where L_{min} is the inductance value at the terminal. The peak value of the current wave is therefore expected to be close to 1000V/

(822 +20) Ω =1.19A, as can be seen in the plot Fig.10-(b) depicting the source current. The corresponding voltage drop across the source internal resistance R_i will be approximately 44V, explaining the curve Fig.10-(c) of the source terminal voltage. The delay time of the equivalent line representing the winding will be close to $\sqrt{L_{average}C_g} \approx 20.85\mu\text{sec}$. This agrees with the approximate time delay of about 2.606 μsec. between the source EMF given by the plot 10-(a) and the current and voltage impulse waves prevailing at $x = 0.125$ per unit depicted in the two plots in Fig.10-(d) and 10-(e), respectively. The approximate value of the line delay corresponds to a natural frequency of about 12 kHz. This is in full agreement with the above mentioned first parallel resonance frequency found for the case of solid earthing, as illustrated by Fig.7.

The significance of taking the nonuniformity of the inductance distribution into account is illustrated by the plot 10-(f) for the current $i_2(t)$ at x = 0.125 per unit computed for a similar hypothetical transformer winding having a uniform distribution constant $L(x)$ = constant = the average inductance = 0.021 mH. This plot is to be compared with the corresponding one 10-(d) for the non-uniform winding. Neglecting the inductance nonuniformity yields a slower transient response with a 4% larger peak current. The instantaneous current at t = 20μsec. is seen to be 0.781A, also larger by about 15.7%.

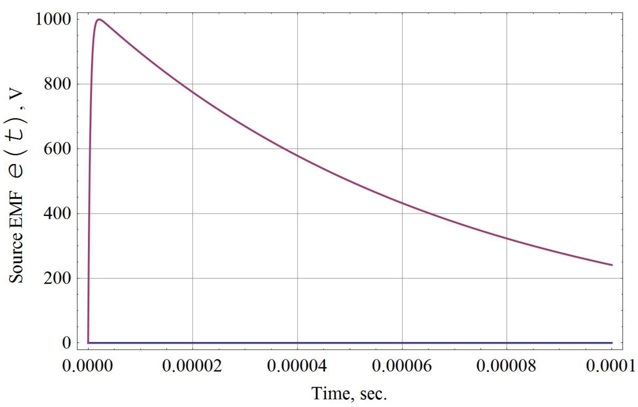

(a) The source EMF

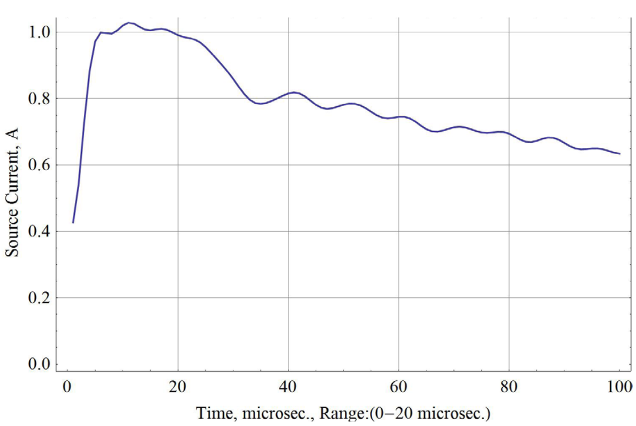

(b) The source current $i_1(t)$

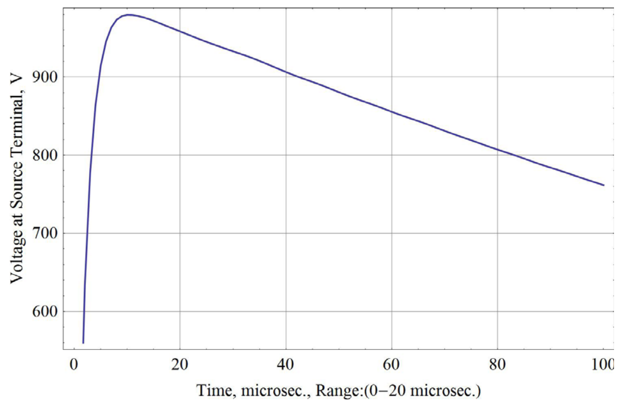

(c)The source terminal voltage $v_1(t)$

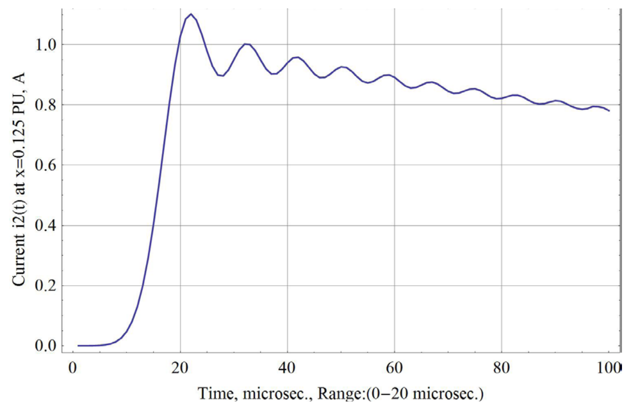

(d)The current $i_2(t)$ at x = 0.125 per unit

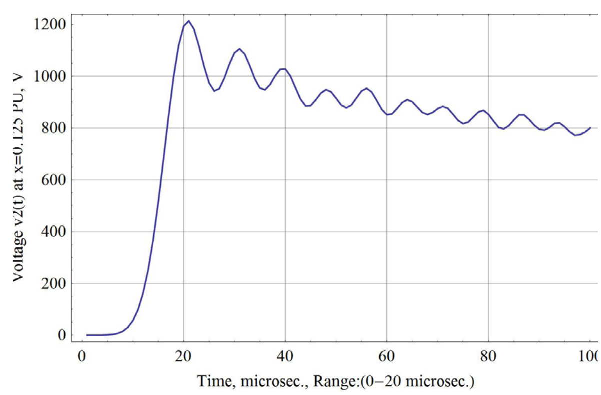

(e)The voltage $v_2(t)$ at x = 0.125 per unit

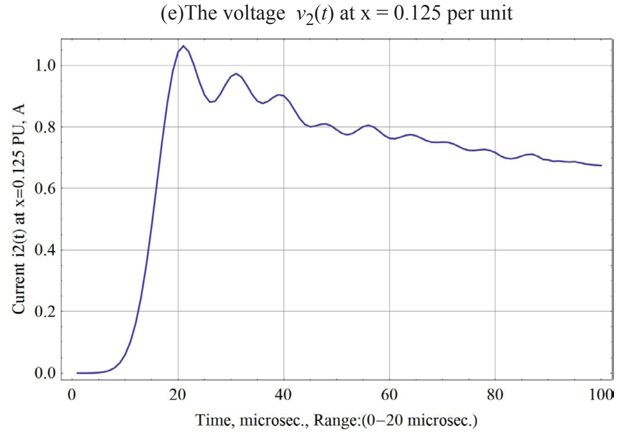

(f) The current $i_2(t)$ at x = 0.125 per unit for a constant $L(x)$ = 0.021 mH.

Fig. 10. The winding's transients due to a 1000V double-exponential voltage impulse

2. Transients Due to a Step Voltage

The two plots in Fig.11 illustrate the winding's transient response to a source of a 1000V step EMF, i.e. $e(t) = 1000\,u(t)$ and $E(s) = 1000/s$. Again, they depict the current and voltage at $x = 0.125$ per unit over the extended time range $0 \le t \le 800$ µsec. The wave reflections at the short-circuited neutral point can be clearly recognized. They are manifested by simultaneous increases in the current and corresponding decreases in the voltage. The current goes asymptotically to its final value 1000/(20+2.2) ≈ 45A and the corresponding final value of the voltage at the same winding point is about 86.7V. The sharp voltage overshoot to about 1200V occurring 4µsec. after switching the source agrees well with the previously discussed plot 10-(e).

IV. VALIDATION OF THE SOLUTION TECHNIQUE

The suggested procedure is validated by its application to a case of a non-uniform inductance distribution for which an exact analytical solution in the *s*-domain is available by using the software *Mathematica*. For simplicity, the case of a lossless winding is considered. The value zero is therefore assigned to the elements G_o, R and G_s of the equivalent circuit. The voltage and current will be denoted V and I, respectively. Applying Kirchhoff's laws and assuming zero time initial conditions, it follows:

$$\frac{dI}{dx} = -V.sC_g \tag{11}$$

and

$$\frac{dV}{dx} = -I.[sC_s + 1/sL(x)]^{-1} \tag{12}$$

with the boundary conditions:
$V(0) = E(s)$ for the terminal input voltage, and $V(1) = 0$ for the solidly-earthed neutral point.

A closed-form solution can be achieved if the following expression for the location-dependent inductance $L(x)$ is assumed:

$$L(x) = a.b^x \tag{13}$$

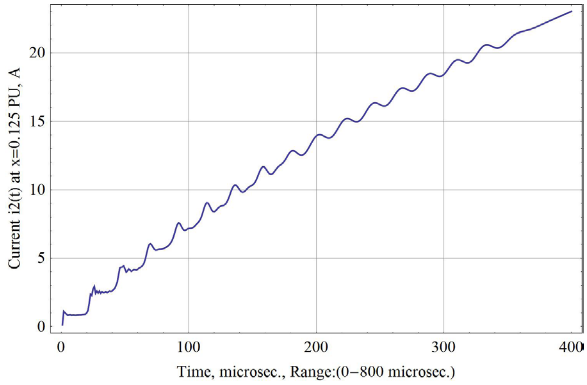

(a) The current $i_2(t)$ at $x = 0.125$ per unit

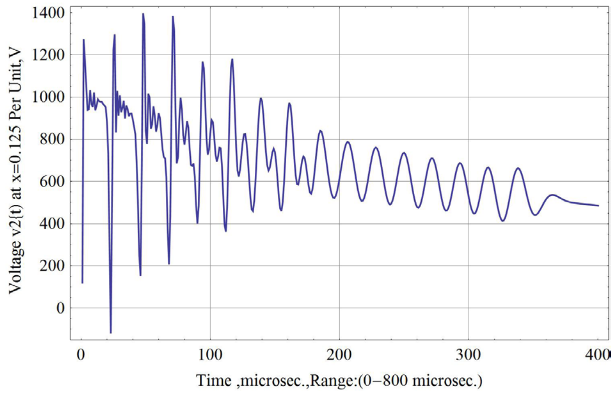

(b) The voltage $v_2(t)$ at $x = 0.125$ per unit

Fig. 11. The winding's transients due to a 1000V step voltage. The neutral point is solidly-earthed.

The numerical values $a = 0.014$ Henries and $b = 2$ are substituted.
For further details on the exact solution, the *Mathematica* documentation should be consulted [15].

The plots (a) and (b) of Fig. 12 depict the dependence of both the magnitude and the imaginary component of the winding's input impedance over the frequency range $0 \le f \le 70$ kHz, respectively. Three parallel and three series resonance frequencies can be recognized. The parallel ones are close to 11.5, 36.5 and 61 kHz, whereas the series

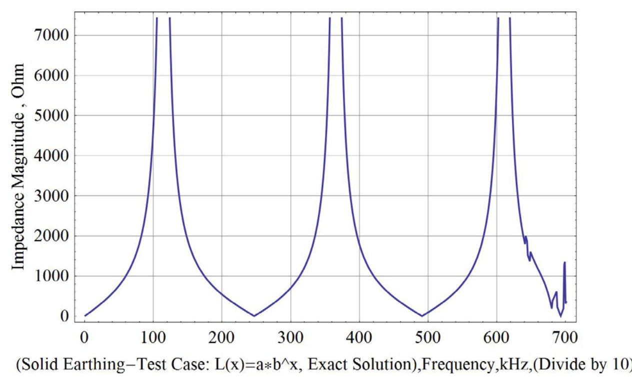

(a) The impedance magnitude

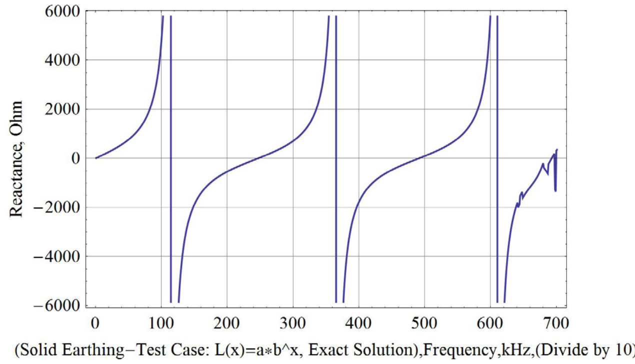

(b) The imaginary part

Fig. 12. The magnitude and the imaginary part of the input impedance as obtained from the exact solution using *Mathematica.*

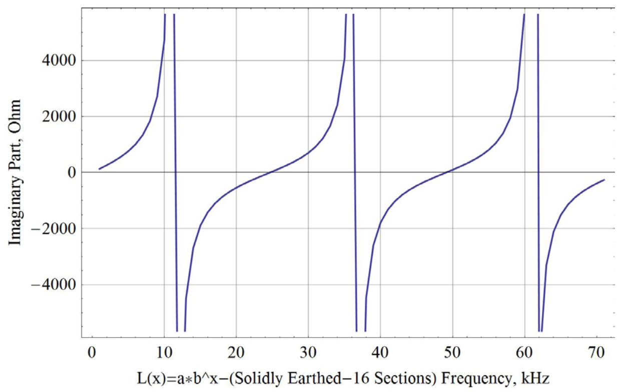

(a) The imaginary part

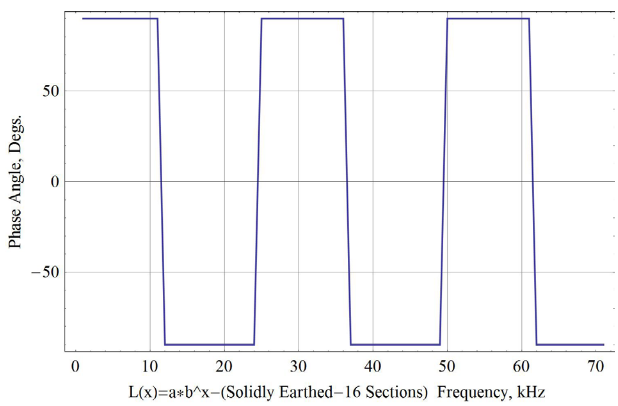

(b) The impedance angle

Fig. 13. The imaginary part and the angle of the input impedance as obtained using the suggested procedure.

resonances occur at the approximate values 24.5, 49 and 70 kHz, respectively. The plot (b) indicates the frequency ranges over which the imaginary part is inductive or capacitive. Since the winding is assumed lossless, the impedance angle can be either $+\pi/2$ or $-\pi/2$.

The information in Fig. 12 should be compared with the corresponding results given by the plots 13-(a) and 13-(b) obtained using the here suggested technique with m = 16 sections. A good agreement can be easily observed for the considered frequency range.

The second validation test will deal with some results in the time domain. Here, the transient response of the lossless winding described by Eq. (13), as obtained using both the exact as well as the suggested procedure will be compared. The considered time range is $0 \leq t \leq 6000$ µsec. The source internal resistance of the 1000V step voltage source is 20Ω, leading to a steady state current of 50A, as both current plots (a) and (c) indicate. It is noticed that both curves are almost identical. The same can be said about the two curves (b) and (d) for the terminal voltage. Both go asymptotically to the expected final value of zero. The results are close to those of a RL–series circuit. The time constant is approximately $(L_{average} / R_{series}) \approx 0.021\text{H}/20\Omega \approx 1050\mu\text{sec}$. It should be noted that the four plots of Fig.14 include superimposed high frequency oscillations of very small amplitudes, similar to those in Figs. 10 and 11.

V. CONCLUSIONS

— A method is suggested for the transient and frequency analysis of transformer windings, taking into account the non-uniform distribution of its series inductance.

— The winding is replaced by a number of cascade connected sections. Each section is represented in the

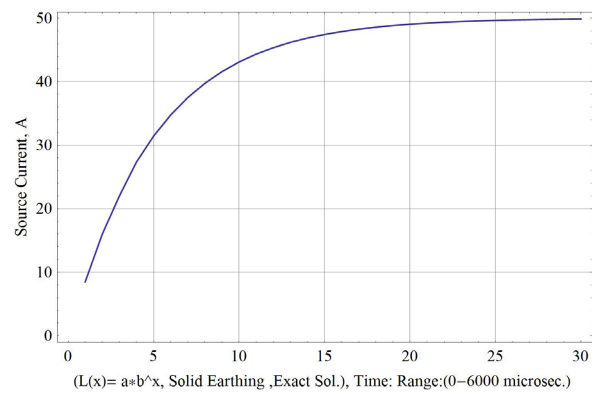

(a) The source current, from the exact solution using *Mathematica*.

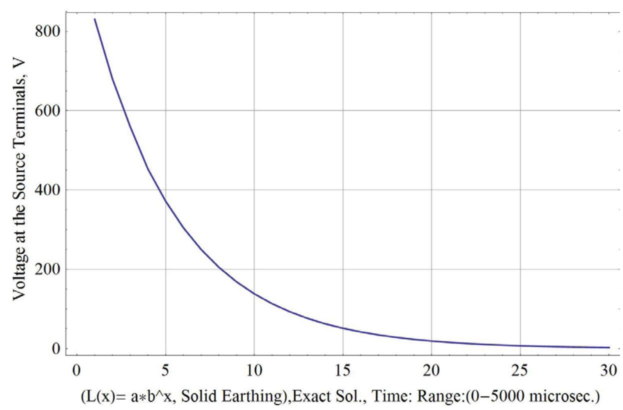

(b) The voltage at the source terminals, from the exact solution using *Mathematica*.

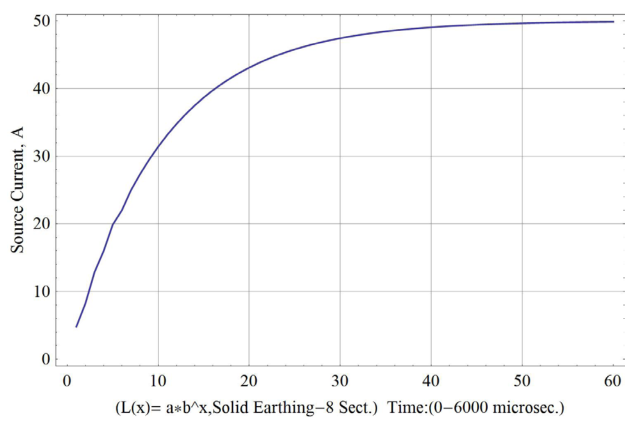

(c) The source current, from the suggested method.

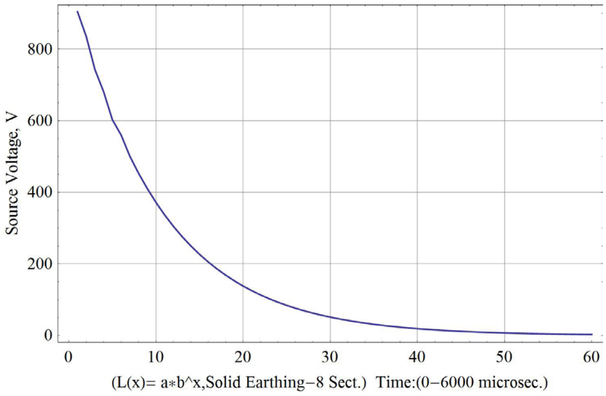

(d) The voltage at the source terminals, using the suggested procedure.

Fig. 14. A comparison of the winding transients resulting from both the exact solution using *Mathematica* (Plots a and b for the current and voltage, respectively) and through the application of the proposed technique (Plots c and d for the current and voltage, respectively).

Laplace s-domain by an equivalent long line. The exact long line theory is applied to determine the section's *ABCD* generalized circuit constants. They are generally not equal for the different sections.

— Analytical expressions for the winding's input impedance as well as for the voltage and current distributions as functions of the complex frequency are derived. The different treatments of the transformer's neutral point are considered. The frequency characteristics are discussed with special emphasis on the resonance phenomena.
— By applying an algorithm for the numerical inverse Laplace transform, the winding's time response for different source voltage waveforms is presented.
— The suggested approach is validated by comparing the results of its application to the corresponding ones of a case study for which exact analytical solutions are available. An agreement of both the frequency and transient responses is observed.
— The method can be easily extended in order to deal with eventual nonuniformities of other winding's equivalent circuit parameters.

REFERENCES

1. Greenwood A.: Electrical Transients in Power Systems. Book, Wiley-Interscience, Second edition, 1991, Chapter 11.
2. Degeneff R.C.: A General Method for Determining Resonances in transformer Windings", IEEE Trans. on PAS, Vol.96, 1977, No.2, pp.423-430.
3. Hosseini S., Vakilian M., Gharehpetian G.: Comparison of Transformer Detailed Models for Fast and Very Fast Transient Studies. IEEE Trans. Power delivery, Vol.23, no.2 pp.733-741, April 2008.
4. Jayaratchagan R., Shriram B.: Impulse Voltage Distribution. International Journal of Engineering Research & Technology (IJERT), Vol. 2 Issue 4, April - 2013, ISSN: 2278-0181, pp. 1203-1207.
5. Saied M.M., AlFuhaid A.S.: Electromagnetic Transients in Line-Transformer Cascade by a Numerical Laplace Transform Technique. IEEE Trans. on PAS, Vol.104, 1985, pp.2901-2909.
6. Saied M.M.: Effect of Cable Sections on the Electromagnetic Transients in Power Networks. J. Electric Machines and Power Systems, 15:17-35, 1988.
7. Saied M.M.: The Transient Response and Frequency Characteristics of Power Transformers Having Non-Uniform Winding Insulation. Paper No. 4453. To be published in J. of Power Electronics and Power Systems, 2014.
8. Saied M.M.: Effect of Transformer Sizes and Neutral Treatments on the Electromagnetic Transients in Transformer Substations. IEEE Trans. on Industry Applications, Vol.31, 1995, No.2, pp. 384-391.
9. Saied M.M., AlFuhaid A.S.: Frequency Response of Two-Winding Transformers Obtained by a Distributed-Parameter s-Domain Method. Journal of Electric Power Components and Systems, Vol.32, 2004, No.8, pp. 755-766.
10. Saied M.M.: New Solution Technique for the Frequency and Transient Response of Transformer Windings with All Inter-Turn Mutual Inductances and Capacitances Included. Paper No. 3143, J. Trends In Electrical Engineering, Volume 3, Issue 1, ISSN: 2249-4774, 2013.
11. Saied M.M.: A Contribution to the Frequency Analysis and the Transient Response of Power Transformers' Windings. submitted for publication in J. Electric Power Components and Systems, 2014.
12. Saied M.M.: On the Transient Response and Frequency Analysis of Transmission Line Towers. ISRN Power Engineering, Hindawi Publishing Corporation, Volume 2013 v(2013), Article ID 874647, 8 Pages. Available at: http://dx.doi.org/10.1155/2013/874647.
13. Predota A., Benesova Z., Koudela L.: Analysis of Transients in Transformer Winding Respecting Space-Varying Inductance. PRZEGLĄD ELEKTROTECHNICZNY (Electrical Review), ISSN 0033-2097, R. 88 NR 7b/ (2012), pp. 220-222.
14. Predota A., Benesova Z.: Fast Transient Overvoltage in Transformer Winding. PRZEGLĄD ELEKTROTECHNICZNY (Electrical Review), ISSN 0033-2097, R. 87 NR 5/2012, pp. 142-145.
15. Wolfram Mathematica Tutorial Collection: Advanced Numerical Differential Equation Solving in Mathematica. Book, Wolfram Research Inc., 2008, available at: http://www.wolfram.com/learningcenter/tutorialcollection/AdvancedNumericalDifferentialEquationSolvingInMathematica/

Mohamed Mostafa Saied
Received the B.Sc. degree (Honors) in Electrical Engineering from Cairo University, Egypt in 1965, then the Dipl.-Ing. and Dr-Ing. Degrees from RWTH Aachen, Germany, in 1970 and 1974. From 1974 to 1983, he was at Assiut University, Egypt. In 1983, he joined Kuwait University where he served as a full professor (1983-2009) and Department Chairman (2002-2007). He spent one-year sabbatical leave (1998) as a Visiting Professor at Cairo University.
Prof. Saied is an IEEE Senior Member.